



**HAL**  
open science

**Microorganism dynamics in a mudflat during rising tide**  
**Microorganism dynamics during a rising tide:**  
**Disentangling effects of resuspension and mixing with**  
**offshore waters above an intertidal mudflat**

Katell Guizien, Christine Dupuy, Pascaline Ory, H el ene Montani e, Hans  
Hartmann, Mathieu Chatelain, Mikha il Karpytchev

► **To cite this version:**

Katell Guizien, Christine Dupuy, Pascaline Ory, H el ene Montani e, Hans Hartmann, et al.. Microorganism dynamics in a mudflat during rising tide Microorganism dynamics during a rising tide: Disentangling effects of resuspension and mixing with offshore waters above an intertidal mudflat. Journal of Marine Systems, 2013, 10.1016/j.jmarsys.2013.05.010 . hal-01248055

**HAL Id: hal-01248055**

**<https://hal.science/hal-01248055>**

Submitted on 26 Dec 2016

**HAL** is a multi-disciplinary open access archive for the deposit and dissemination of scientific research documents, whether they are published or not. The documents may come from teaching and research institutions in France or abroad, or from public or private research centers.

L'archive ouverte pluridisciplinaire **HAL**, est destin ee au d ep ot et  a la diffusion de documents scientifiques de niveau recherche, publi es ou non,  emanant des  tablissements d'enseignement et de recherche fran ais ou  trangers, des laboratoires publics ou priv es.

1 **Running title: Microorganism dynamics in a mudflat during rising tide**

2

3

4 **Microorganism dynamics during a rising tide: Disentangling effects of resuspension and**  
5 **mixing with offshore waters above an intertidal mudflat**

6

7 **Katell Guizien<sup>1†\*</sup>, Christine Dupuy<sup>2†</sup>, Pascaline Ory<sup>2</sup>, H  l  ne Montani  <sup>2</sup>, Hans**  
8 **Hartmann<sup>2</sup>, Mathieu Chatelain<sup>1\*\*</sup>, Mikha  l Karpytchev<sup>2</sup>**

10 1. **Laboratoire d'Ecog  ochimie des Environnements Benthiques, Observatoire**  
11 **Oc  anologique de Banyuls-sur-Mer, UMR8222, CNRS-Universit   Pierre et**  
12 **Marie Curie, rue du Fontaul  , 66650 Banyuls-sur-Mer, France**

13 2. **Littoral, Environnement et Soci  t  s (LIENSs), Universit   de La Rochelle, UMR**  
14 **7266 CNRS-ULR, 2 rue Olympe de Gouges, 17000 La Rochelle Cedex, France**

15

16 **† These authors contributed equally to this work.**

17 **\*Corresponding author: [guizien@obs-banyuls.fr](mailto:guizien@obs-banyuls.fr), Tel: +33 (0) 468 887 319, Fax: +33 (0)**  
18 **468 887 395**

19 **\*\* Present address: Deltares, P.O. Box 177, 2600 MH Delft, The Netherlands**

20

21

22 **Keywords: microorganisms dynamics, benthic-pelagic coupling, resuspension, tidal mudflat**

23

24

25

26

27

1

2

1

28 **Abstract**

29 Resuspension of microphytobenthic biomass that builds up during low tide has been  
30 acknowledged as a major driver of the highly productive food web of intertidal mudflats. Yet,  
31 little is known about the contribution to pelagic food web of the resuspension of other  
32 microorganisms such as viruses, picoeukaryotes, cyanobacteria, bacteria, nanoflagellates, and  
33 ciliates, living in biofilms associated with microphytobenthos and surficial sediment. In the  
34 present study, a novel approach that involves simultaneous Lagrangian and Eulerian surveys  
35 enabled to disentangle the effects of resuspension and mixing with offshore waters on the  
36 dynamics of water column microorganisms during a rising tide in the presence of waves.  
37 Temporal changes in the concentration of microorganisms present in the water column were  
38 recorded along a 3 km cross-shore transect and at a fixed subtidal location. In both surveys,  
39 physical and biological processes were separated by comparing the time-evolution of  
40 sedimentary particles and microorganisms concentrations. During a rising tide, sediment  
41 erosion under waves action occurred over the lower and upper part of the mudflat, where  
42 erodibility was highest. Although erosion was expected to enrich the water column with the  
43 most abundant benthic microorganisms, such as diatoms, bacteria and viruses, enrichment  
44 was only observed for nanoflagellates and ciliates. Grazing probably overwhelmed erosion  
45 transfer for diatoms and bacteria, while adsorption on clayed particles may have masked the  
46 expected water column enrichment in free viruses due to resuspension. Ciliate enrichment  
47 could not be attributed to resuspension as those organisms were absent from the sediment.  
48 Wave agitation during the water flow on the mudflat likely dispersed gregarious ciliates over  
49 the entire water column. During the rising tide, offshore waters imported more autotrophic,  
50 mainly cyanobacteria genus *Synechococcus* sp. than heterotrophic microorganisms, but this  
51 import was also heavily grazed. Finally, the water column became a less heterotrophic  
52 structure in the subtidal part of the semi-enclosed bay, where mixing with offshore waters  
53 occurs (50% decrease), compared to the intertidal mudflat, when resuspension occurs. The

54 present study suggests that this differential evolution resulted predominantly from dilution  
55 with offshore waters less rich in heterotrophic microorganisms. Indeed, any input of  
56 microorganisms accompanying physical transfers due to bed erosion or offshore waters  
57 mixing was immediately buffered, probably to the benefit of grazers.

58

## 59 **1. Introduction**

60 The productivity of coastal systems, especially intertidal mudflats, and their capacity  
61 to enrich adjacent terrestrial and marine zones through trophic pathways (i.e. export by mobile  
62 consumers) and hydrodynamic pathways (i.e. waves, wave-generated currents, estuarine  
63 currents and tides) is now common knowledge. The biological productivity of intertidal  
64 mudflats is due to the intense activity of benthic microorganism communities. During  
65 emersion, epipellic diatoms (microphytobenthos, MPB) form a biofilm (up to 20 mg  
66 chlorophyll *a* m<sup>2</sup>) in the top centimeter layer of a mud surface (Blanchard and Cariou-Le Gall  
67 1994; Blanchard et al. 1997; Herlory et al. 2004). Prokaryote communities are associated with  
68 this biofilm, and bacterial production (secondary production) can be as high or even higher  
69 than MPB production (primary production) (Cammen 1991; Garet 1996; Van Duyl and Kop  
70 1994). Bacterial concentration is generally about 10<sup>9</sup> cells per cm<sup>3</sup> in a mudflat (Schmidt et al.  
71 1998). Nanoflagellate concentrations range from 100 to several million cells per mL of  
72 sediment (Gasol 1993), with greater concentrations in surficial sediment (Alongi 1991).  
73 Conversely, ciliates are more abundant in fine sand (Fenchel 1969; Kemp 1988; Epstein  
74 1997) compared to muddy sediment enriched with organic matter (Giere 1993). Viruses are  
75 also abundant in marine sediments (Danovaro et al. 2008).

76 Resuspension of microorganisms living either in the pore water of surficial sediment  
77 or attached to surficial sedimentary particles have been reported under tidal currents at  
78 subtidal sites (Shimeta et al. 2002). Large tidal currents in macrotidal bays are likely to induce  
79 unconsolidated sediment resuspension (Mehta et al. 1989). Yet, resuspension of sediment

80 across intertidal mudflats, where recurrent desiccation promoted sediment consolidation  
81 (Anderson and Howel 1984), generally requires higher shear stress than those induced by tidal  
82 current and has been mainly attributed to wave action (Bassoulet et al. 2000; French et al.  
83 2008). However, sediment erodibility thresholds may be significantly reduced (bed friction  
84 velocity below  $3 \text{ cm s}^{-1}$ ) due to macrofaunal bioturbation activity (Orvain et al. 2007).

85 Resuspended microorganisms may greatly affect pelagic and benthic food webs.  
86 Resuspended diatoms and autotrophic nanoflagellates may alter phytoplankton community  
87 structure, enhance phytoplankton biomass and modify the size structure of primary producers,  
88 ultimately modifying microbial food web function (Marquis et al. 2007; Ory et al. 2010). In  
89 addition, resuspended heterotrophic cells, such as nanoflagellates, prokaryotes (bacteria and  
90 archaea) and viruses, can affect the function of the food web, and favour the microbial loop or  
91 the viral shunt (Wainright 1987; Garstecki et al. 2002; Seymour et al. 2007). Furthermore,  
92 some of these resuspended microorganisms may be used as food resources for  
93 mesozooplankton and benthic suspension feeders (Carlson et al. 1984), such as oysters  
94 (Dupuy et al. 2000) and bivalve mollusks (*Scrobicularia plana*) (Hughes 1969).

95 Many studies have investigated the dynamics of the MPB biomass, including  
96 resuspension of these microorganisms (Lucas et al. 2000; Shimeta et al. 2002; Guarini et al.  
97 2008). Some studies have qualitatively and quantitatively evaluated the resuspension of other  
98 microorganisms present in the intertidal mudflat. Protist and bacteria resuspension thresholds  
99 have been quantified at a subtidal coastal site with *in situ* flumes and sampling of the benthic  
100 boundary layer during tidal accelerations (Shimeta and Sisson 1999; Shimeta et al. 2002).  
101 Shimeta et al. (2003) studied the resuspension of benthic protists at subtidal coastal sites with  
102 differing sediment compositions. Other studies have explored the effects of sediment  
103 resuspension on a coastal planktonic microbial food web, either experimentally (Garstecki et  
104 al. 2002; Pusceddu et al. 2005; Wu et al. 2007) or in the field (Grémare et al. 2003). However,  
105 in field studies, resuspension is often accompanied by other physical processes, such as river

106 flooding and tidal rise, which require adapted sampling strategies to separate the contribution  
107 of each process.

108 In the current study, we applied a novel approach based on two simultaneous  
109 Lagrangian and Eulerian field surveys to disentangle the effect of resuspension and mixing  
110 with offshore waters on the dynamics of water column microorganisms during a tidal flow.  
111 The time-evolution of microorganisms, including viruses, autotrophic protists, heterotrophic  
112 protists and prokaryotes present in the water column, were carried out at one fixed location  
113 (Eulerian) and one mobile station (Lagrangian) in the Marennes-Oleron bay (French Atlantic  
114 coast). In both surveys, physical and biological processes were separated by comparing the  
115 time-evolution of suspended sediment particles and microorganisms concentrations.

116

## 117 **2. Methods**

### 118 *2.1 Study site and sampling strategy*

119 The study was carried out during the afternoon rising tide (tidal amplitude of 3.8 m) in  
120 the Bay of Marennes-Oléron (BMO) on 24 July, 2008. Located between the mainland French  
121 Atlantic coast and Oléron Island, BMO is a macrotidal bay with a tidal range up to 6 m during  
122 spring tides. This macrotidal system is influenced by continental inputs, mainly from the  
123 Charente River to the north of the BMO (monthly average discharge was  $30 \text{ m}^3 \text{ s}^{-1}$  in July  
124 2008, slightly less than the median value of  $40 \text{ m}^3 \text{ s}^{-1}$  over the last ten years). The BMO  
125 covers  $170 \text{ km}^2$ , of which  $60 \text{ km}^2$  are intertidal mudflats. The Brouage mudflat is  $>4 \text{ km}$  wide,  
126 and its sediment consists of silt and clay particles (95% of  $<63 \mu\text{m}$ , median grain size  $d_{50} = 10$   
127  $\mu\text{m}$ ). Triplicate samples of the first 1 cm layer of sediment were taken at the end of low tide in  
128 the upper region of the mudflat (Fig. 1). Only concentrations of bacteria and viruses were  
129 assessed in surficial sediment. Two simultaneous field surveys (Lagrangian and Eulerian)  
130 were carried out to separate the effect on the dynamics of water column microorganisms of  
131 resuspension and mixing with offshore waters during tidal flow. Adopting a Lagrangian

132 strategy avoided transport flux gradients that occur in an Eulerian survey. Such transport flux  
133 gradients occur as the water level changes in an Eulerian survey and pelagic concentrations  
134 are generally expected to be mixed (diluted or enriched) by offshore waters in proportion to  
135 water depth. Conversely, no mixing (especially dilution) is expected in a Lagrangian survey,  
136 where the water level remains constant. In both types of surveys, temporal changes in  
137 concentrations of a group of organisms, or particulate or dissolved matter that depart from  
138 these expectations indicate an imbalance between the many biogeochemical processes that  
139 potentially affect this group (Fig. 2). For particulate matter or living low-motility cells, an  
140 overall increase in concentration indicates that either benthic resuspension or population  
141 growth dominate, whereas a decrease indicates that either sedimentation mediated by sorption  
142 on matters or population decay (e.g. grazing) dominates.

143 Before organizing the field measurements, a 2D barotropic model was used to compute  
144 using a backward procedure the trajectory of a drifter reaching the shore in the northern part  
145 of the Brouage mudflat (Fig. 1) at the end of the rising tide (Nicolle and Karpytchev 2007).  
146 The model used a high resolution, finite element grid and TELEMAC software to solve the  
147 depth integrated equations of Saint Venant (Hervouet and Van Haren 1994; Hervouet 2007).  
148 The Eulerian subtidal station was located at the origin of the drifter trajectory for the case of a  
149 no-wind tidal circulation in the BMO (Fig. 1).

150 The Lagrangian survey consisted of tracking a submerged buoy following the tidal front  
151 during the first 2 h 45 min of the rising tide over the intertidal Brouage mudflat, between  
152 15:45 h and 18:30 h local time (Fig. 1). The tidal front travelled roughly at a speed of 30 cm s<sup>-1</sup>.  
153 Cylindrical drifters (46 cm in diameter and 50 cm in height) were used to track the  
154 advancing tidal currents into the BMO. Drifter walls were made of plastic film wrapped  
155 around a thin metal rod armature and a 10 cm plastic spherical buoy was fixed on its top. The  
156 drifter was completely immersed to be directed by surface currents and the buoyant sphere  
157 which emerged from water was used to keep track of the drifter position. The drifter was

158 tracked using a flatboat which engine was stopped and left drifting for at least 5 min before  
159 sampling in order to avoid bottom resuspension artefacts. Water samples were obtained at five  
160 different stations along the 3 km cross-shore transect (Fig. 1) on 24 July, 2008. Due to rapid  
161 drifting when the engine was stopped before sampling, first Lagrangian station was already  
162 located a 100 m away from the Eulerian station. Water depth varied little during the  
163 Lagrangian survey, ranging from 40 to 70 cm. One sample was collected in the middle of the  
164 water column at each station using a 1 L plastic bottle attached to a graduated stick. Short  
165 wave agitation combined with limited water depth during the Lagrangian survey did not allow  
166 sampling with an open-ended Nisking bottle, so a smaller closed-bottom bottle was used.  
167 However, sampling bias due to accumulation of settling particles in a closed-bottom bottle  
168 was reduced by a fast sampling lasting less than a few seconds and by introducing the bottle  
169 upside down. Since wave length was greater than water depth, short wave agitation ensured  
170 sufficient mixing over the entire water depth, making it safe to assume no stratification for all  
171 sampled microorganisms (except very close to the bottom) occurred during the Lagrangian  
172 survey. Each individual sample was divided into multiple aliquots to perform replicate counts.  
173 Immediately before preparation of aliquots, each sample was gently agitated and subsampling  
174 was performed very quickly to prevent sedimentation.

175 The Eulerian survey consisted of sampling the water column with horizontal 3 L Niskin  
176 bottles at the same subtidal spot during the rising tide, starting at low tide (Fig. 1). Water  
177 depth at the sampling station increased from 1.10 m at the beginning of the survey to 3.1 m at  
178 the end of sampling. Three water samples were taken 0.5 m below the surface and 0.5 m  
179 above the bottom of the water column during the first 2 h 45 min of the rising tide on 24 July,  
180 2008. Aliquots of each sample were prepared as described above.

181

182 Mean and standard deviation of all variables at the beginning of the rising tide were  
183 computed from the three samples taken at time zero of the Eulerian and Lagrangian surveys.



184 An 80% confidence interval for this initial measurement was computed using a Student law  
185 ( $t_{n-1}(1-\alpha)=1.886$ ,  $\alpha=10\%$ ). Evolution of the concentration of particulate inorganic matter  
186 (PIM) and each microorganism at the Eulerian site were predicted using on a simple mixing  
187 model based on water depth evolution, assuming that the (1) water column was well-mixed at  
188 the Eulerian site and (2) concentration of PIM or each microorganism in incoming waters  
189 could be estimated from the average concentration measured to the north of the BMO basin  
190 taken before the experiment then 15 days after. The average concentration PIM or each  
191 microorganism expected after mixing with offshore waters during tidal flow,  $C_t$ , was  
192 calculated during the Eulerian survey for sampling times after 1h15min and 2h45min as  
193 follows:

$$C_t = C_0 \frac{h_0}{h_t} + C_{ext} \left[ 1 - \frac{h_0}{h_t} \right]$$

194  
195 where  $C_0$  is the average concentration at time zero of the Eulerian survey,  $h_0$  is the water depth  
196 at this time,  $h_t$  is the water depth at time  $t$  and  $C_{ext}$  is the average offshore concentration. An  
197 80% confidence interval for this predicted value was build applying a Student law ( $n=3$ ) using  
198 standard deviation of  $C_0$  and  $C_{ext}$ . Backward trajectories reaching the Eulerian survey  
199 sampling station after 1h15min and 2h45min were also computed for the the case of no-wind  
200 tidal circulation in the BMO with the 2D barotropic model and indicated that offshore waters  
201 most probably came from the northern entrance of the BMO, west of the Charente river  
202 mouth (Fig. 1). In the absence of river flooding over the summer period, the impact of the  
203 Charente river on the pelagic ecosystem was limited at this location (Stanisière, personal  
204 communication), allowing us to assume that the concentration in the north of the BMO was  
205 spatially uniform (Ory et al. 2010). Offshore concentrations at 0.5 m below the surface were  
206 measured on July 12 and 29, 2008, at a subtidal station roughly 15 km northwest of the BMO  
207 (water depth = 17 m, 46.1153°N, 01.4139°Wr). Values for  $C_{ext}$  on July 24 were interpolated  
208 by taking the mean between offshore concentrations at the two dates (see Table 1) and

209 uncertainty on offshore concentrations on the day of the survey was accounted for using  
210 standard deviation between the two dates. Variability estimate based on those two days are  
211 similar to within day variability (H. Montanié, personal communication) and to within  
212 summer variability (Ory et al., 2010) in the north of BMO basin.

213

## 214 *2.2 Physical forcings*

215 Hydrological parameters, such as temperature and salinity, were recorded on board  
216 with multi-parameter probes (YSI 6600EDS-M) during the Eulerian survey. Average wind  
217 speed and direction were measured every hour by Météo-France at the La Rochelle  
218 Aéroport meteorological station (46.1733°N, 1.1883°W, roughly 20 km north of the BMO).  
219 A single-point Nortek acoustic Doppler velocimeter (ADV) was used to measure the 3D  
220 velocity at 15.6 cm a.b. (above bottom, outside the wave boundary layer which thickness  
221 yielded 3 cm at maximum, Fredsoe and Deigaard,1992) and pressure as soon as the tide level  
222 was higher than 50 cm at the location 45.9161°N, 1.0890° W (Fig. 1). Thus, ADV data  
223 collection was interrupted during low tide from 12:45 h to 18:15 h on 24 July, 2008.  
224 Measurements consisted of 2 min 30 s time series recorded at a frequency of 32 Hz every 15  
225 min for the three velocity components and pressure. Turbulent Reynolds shear stress outside  
226 the wave boundary layer were computed as the covariance of horizontal and vertical velocity  
227 deviations from the mean flow after removing wave-induced velocities. Wave-induced  
228 velocities were computed by applying a 0.5 Hz low pass filtering on raw velocity  
229 measurements (Guizien et al. 2010). Assuming a logarithmic boundary layer, bed shear stress  
230 associated with tidal current was then linearly extrapolated to the bed using Reynolds shear  
231 stress measured at 15.6 cm a.b. and zero Reynolds shear stress at the free surface.

232 Wave density spectra were computed from pressure time series sampled at 4 Hz and  
233 used to derive the wave parameters (i.e. mean spectral period,  $T_m$ , and significant height,  $H_s$ )  
234 over the Brouage mudflat. Assuming that the wave field was uniform over the mudflat, wave

235 orbital velocities at 40 cm a.b. were derived from  $T_m$  and  $H_s$ , according to the linear wave  
236 theory for varying water depths,  $D$ , at the Eulerian survey site and for a constant water depth  
237 of 40 cm during the Lagrangian survey. Time-dependent bed shear stress associated with a  
238 sine wave with these orbital velocities are described by their maximum value and average  
239 value over a wave period (half the maximum value) using Guizien and Temperville (1999)  
240 parameterization. Bed roughness was assumed to be 0.5 cm based on the bioroughness height,  
241 which could be visually estimated on the mudflat. By definition, bed friction velocity ( $u^*$ )  
242 either due to waves or to the tidal current is the square root of the bed shear stress divided by  
243 seawater density.

244

### 245 *2.3 Particulate inorganic matter (PIM)*

246 Total particulate matter was measured as previously described by Aminot and  
247 Chaussepied (1983). Filters were combusted at 490°C for 2 h to eliminate organic carbon  
248 content and then weighed. A water sample (from 300 to 1000 mL) was filtered onto a  
249 Whatman GF/C (47 mm in diameter) under <10 mm Hg vacuum pressure. After sample  
250 filtration, each filter was rinsed twice with MilliQ water to remove salt, dried at 60°C for 12 h  
251 then weighed to measure total particulate matter. Filters were combusted at 490°C for 2 h to  
252 eliminate organic carbon content and then weighed to determine content of particulate  
253 inorganic matter (PIM).

254

### 255 *2.4 Enumeration of microorganisms*

256 Water samples (up to 50 mL) were stained with 1% alkaline Lugol's solution to  
257 visualise microplanktonic cells, such as diatoms, dinoflagellates and ciliates, ranging from 20  
258 to 200  $\mu\text{m}$ . Microphytoplanktonic cells were counted using an Utermöhl settling chamber  
259 (Hydro-Bios® combined plate chambers) under an inverted microscope. Taxonomic  
260 determination was carried out in accordance with systematics literature (Nezan, 1996; Ricard,

261 1987; Sournia, 1986), and benthic species were differentiated from planktonic species based  
262 on knowledge of the habitat.

263 For nanoplanktonic cells (3 to 15  $\mu\text{m}$ ), water samples (up to 20 mL) were fixed using  
264 1% paraformaldehyde then stained with DAPI (4',6'-diamidino-2-phénylindole). Autotrophic  
265 nanoflagellates (ANF) and heterotrophic nanoflagellates (HNF) were counted as previously  
266 described by Dupuy et al. (1999), which was a modified methodology from Haas (1982),  
267 Caron (1986), and Sherr et al. (1994).

268 For picoeukaryotes (or picophytoeukaryotes) and *Synechococcus* (1 to 2  $\mu\text{m}$ ), water  
269 samples (3 mL) were fixed using 2% formaldehyde, frozen in liquid  $\text{N}_2$ , and counted using a  
270 FACSCan flow cytometer (Bd-Bioscience) as previously described by Marie et al. 2000.

271 For viruses (20 nm), triplicate water samples (3 mL) were fixed in filtered 2%  
272 formaldehyde and stored for less than a day at 4°C. Samples were then filtered through 0.02  
273  $\mu\text{m}$  Anodiscs (25 mm, Whatman) and counted using epifluorescence microscopy after  
274 staining for 30 min with Sybr Green I (Noble and Fuhrman, 1998). Viruses were counted in at  
275 least 15 random fields of view under blue excitation (Zeiss Axioskop 1000x). Only free  
276 viruses were enumerated.

277 For bacteria (1 to 2  $\mu\text{m}$ ), triplicate water samples (3 mL) were fixed with filtered 2%  
278 formaldehyde and stored for less than a day at 4°C. Samples were filtered through 0.02  $\mu\text{m}$   
279 Anodiscs (25mm, Whatman). Samples were enumerated using epifluorescence microscopy  
280 after staining for 30 min with Sybr Green I (Noble and Fuhrman 1998). Bacteria were counted  
281 in at least 15 random fields of view under blue excitation (Zeiss Axioskop 1000x). Free  
282 bacteria were counted with a fixed focalisation on the filter surface while attached bacteria on  
283 aggregates deposited on the filter were screened by varying focal distance.

284 For each group of autotrophic or heterotrophic organisms, biomass was calculated  
285 using conversion factor for cell to carbon content (Table 2) multiplied by abundance.

286

## 287 **3. Results**

### 288 *3.1 Physical forcings*

289 On 24 July, a thermal wind in the morning turned from the southeast (land) to the west  
290 (sea), reaching a maximum speed of  $8.7 \text{ m s}^{-1}$  around low tide at 15:00 h (Fig. 3a). Short  
291 period waves, with a mean period ranging from 2 to 4 s, started growing under wind action  
292 after 11:00 h during ebb tide. At 12:30 h, when the ADV emerged, significant wave height  
293 was already 0.15 m and had increased up to 0.2 m at 18:30 h when ADV was submerged  
294 again at the end of the rising tide (Fig. 3a). Given the slight decrease in wind speed after  
295 15:00 h and based on personal observation, wave height was at least 0.2 m during the survey  
296 period from 15:45 h to 18:30 h. Therefore, a wave height of 0.2 m was used to estimate bed  
297 friction velocity caused by waves. Maximum and mean bed friction velocity due to waves  
298 were at least  $4.5 \text{ cm s}^{-1}$  and  $3.2 \text{ cm s}^{-1}$ , respectively, during the Lagrangian survey under 0.4 m  
299 water depth. In contrast, maximum and mean bed friction velocities due to waves were less  
300 than  $2 \text{ cm s}^{-1}$  and  $1.4 \text{ cm s}^{-1}$ , respectively, when the Eulerian survey started at low tide. These  
301 values continuously decreased to  $0.5 \text{ cm s}^{-1}$  and  $0.35 \text{ cm s}^{-1}$ , respectively, as the water level  
302 rose (Fig. 3b). Bed friction velocity induced by the tidal current reached a maximum value of  
303  $1.3 \text{ cm s}^{-1}$  when the tidal flow arrived at the ADV location (water depth of 0.5 m) and rapidly  
304 decreased to less than  $0.5 \text{ cm s}^{-1}$  during the rest of the rising tide over the intertidal mudflat.

305

### 306 *3.2 Changes in the concentration of particulate inorganic matter during the Eulerian* 307 *and Lagrangian surveys*

308 PIM concentration displayed a large spatial variability at the beginning of the rising tide  
309 surveys (Fig. 4), with a value that was twice as high in the subtidal site ( $300 \text{ mg L}^{-1}$ )  
310 compared to the first Lagrangian sampling station ( $140 \text{ mg L}^{-1}$ ). However, at the end of the  
311 Lagrangian survey, the PIM concentration had increased more than five-fold, up to  $1180 \text{ mg}$   
312  $\text{L}^{-1}$ , largely overpassing the 80% confidence interval around the initial average concentration.

313 Moreover, PIM concentration steadily increased at an average rate of  $0.11 \text{ mg L}^{-1} \text{ s}^{-1}$  as tidal  
314 flow progressed over the mudflat (Fig. 4). Meanwhile, the rate of increase in the PIM  
315 concentration was not constant throughout the survey, reaching  $0.18 \text{ mg L}^{-1} \text{ s}^{-1}$  during the first  
316 hour, falling to  $0.02 \text{ mg L}^{-1} \text{ s}^{-1}$  during the next 40 min and again increasing to  $0.12 \text{ mg L}^{-1} \text{ s}^{-1}$   
317 for 30 min before falling again to  $0.05 \text{ mg L}^{-1} \text{ s}^{-1}$  during the last 30 min. Assuming a uniform  
318 vertical PIM concentration over the 0.4 m water depth due to strong wave agitation, erosion  
319 rates decreased from  $460 \text{ mg m}^{-2} \text{ s}^{-1}$  in the lower part of the mudflat during the first hour to  $60$   
320  $\text{mg m}^{-2} \text{ s}^{-1}$  in the middle part of the mudflat during the next 40 min and increased again to  $300$   
321  $\text{mg m}^{-2} \text{ s}^{-1}$  during the next 30 min. In contrast, in the Eulerian survey, PIM concentration  
322 decreased, with values remaining within the 80% confidence interval of predicted dilution by  
323 offshore waters (Fig. 4).

324

### 325 *3.3 Changes in the concentration of autotrophic microorganisms during the Eulerian* 326 *and Lagrangian surveys*

327 The dynamics of the various taxa of autotrophic microorganisms counted during the  
328 Lagrangian and Eulerian surveys was compared to initial concentration and predicted changes  
329 by mixing with offshore waters, respectively. At the beginning of both surveys, two third of  
330 diatoms were benthic species. This proportion increased during the Lagrangian survey to  
331 nearly 80%. In the Eulerian survey, this proportion decreased to less than 20%, reflecting the  
332 differential effect of resuspension and mixing with offshore waters on water column  
333 microorganism dynamics. Although changes in benthic diatom concentration during the  
334 Lagrangian survey suggested alternate phases of gain in the lower and upper parts of the  
335 mudflat, where erosion was the greatest, and loss in the middle regions of the mudflat, none of  
336 these changes were beyond the 80% confidence interval of the initial concentrations  
337 determined at the beginning of the survey (Fig. 5a). However, the decrease in benthic diatom  
338 concentration was not statistically significant. In contrast, a predicted significant increase in

339 pelagic diatoms was observed during the Eulerian survey. During the Lagrangian survey,  
340 changes in pelagic diatoms concentration were again not statistically significant given the  
341 large variability observed at the beginning of survey (Fig. 5b).

342 Smallest autotrophs were mainly comprised of ANF ( $0.6$  to  $1 \times 10^4$  cells  $\text{mL}^{-1}$ ) in both  
343 surveys, whereas picophytoeukaryotes and *Synechococcus* sp. (e.g. cyanobacteria) displayed  
344 very low concentrations (Fig. 5b-d). During the Lagrangian survey, ANF concentration nearly  
345 doubled during the first 1h15 min, departing from 80% confidence interval around value  
346 when surveys started, and then decreased during the next hour (Fig. 5b). During the Eulerian  
347 survey, ANF concentration displayed opposite dynamics at the surface and at the bottom. In  
348 any case, by the end of the survey, values at the surface and at the bottom overpassed the 80%  
349 confidence interval around values predicted from dilution with offshore waters.

350 Picoeukaryotes concentration steadily decreased during the Lagrangian survey.  
351 However, this trend was not statistically significant given the large variation coefficient at the  
352 beginning of survey (Fig. 5c). During the Eulerian survey, picoeukaryote concentration  
353 displayed opposite dynamics at the surface and at the bottom, increasing at the surface and  
354 decreasing at the bottom (Fig. 5c). However, values were never outside the large 80%  
355 confidence interval around values predicted from mixing with offshore waters.

356 The concentration of *Synechococcus* sp. remained fairly constant ( $4.5 \times 10^3$  cells  $\text{mL}^{-1}$ )  
357 during both surveys (Fig. 5d), with values lower than the 80% confidence interval of  
358 predicted mixing by offshore waters.

359

360 *3.4 Changes in the concentration of heterotrophic microorganisms during the*  
361 *Eulerian and Lagrangian surveys*

362 During the Lagrangian survey, free virus concentration steadily decreased from  $1.2 \times$   
363  $10^7$  particles  $\text{mL}^{-1}$  to  $7 \times 10^6$  particles  $\text{mL}^{-1}$  (Fig. 6a). However, this decrease was not  
364 statistically significant. During the Eulerian survey, free virus concentration at the surface

365 steadily decreased within the 80% confidence interval of predicted dilution by offshore  
366 waters. Conversely, at the bottom, free virus concentration significantly increased during the  
367 first 1h15 min, reaching a value of  $1.8 \times 10^7$  viruses  $\text{mL}^{-1}$ . This value was out of the 80%  
368 confidence interval around values predicted from dilution by offshore waters and even out of  
369 the 80% confidence interval around value when survey started. However, free viruse  
370 concentration at the bottom decreased during the next 1h30 min, reaching a value of  $4 \times 10^6$   
371 viruses  $\text{mL}^{-1}$ , which was within the 80% confidence interval around values predicted from  
372 dilution by offshore waters.

373 Free bacteria dynamics were similar to free virus dynamics during both surveys (Fig.  
374 6b). For attached bacteria concentration, no significant change was observed during the  
375 Lagrangian survey ( $6\text{--}8 \times 10^6$  cells  $\text{mL}^{-1}$ ), while concentration decreased during the Eulerian  
376 survey by one order of magnitude, which was still within the 80% confidence interval of  
377 predicted dilution with offshore waters (Fig. 6c).

378 The dynamics of HNF was similar to the ANF dynamics in the both surveys. During the  
379 Lagrangian survey, HNF concentration increased steadily over the first 2 h10 min to almost  
380 twice the concentration measured at the start of the survey ( $3 \times 10^3$  cells  $\text{mL}^{-1}$ ), but then  
381 decreased during the last 30 min (Fig. 6d). During the Eulerian survey, HNF concentration  
382 displayed opposite dynamics at the bottom and at the surface, but both values remained within  
383 the 80% confidence interval around surveys initial value and the large 80% confidence  
384 interval around values predicted from mixing with offshore waters ( $1.3 \times 10^3$  cells  $\text{mL}^{-1}$ ).

385 During the Lagrangian survey, ciliate concentration doubled along the transect to values  
386 greater than the 80% confidence interval estimated when the survey began (Fig. 6e). During  
387 the Eulerian survey, ciliate concentration decreased at the bottom and at the surface more than  
388 expected from dilution with offshore waters at the bottom (i.e. lower than the 80% confidence  
389 interval).

390



391 In summary, the water column only became significantly enriched with nanoflagellates  
392 (autotrophs and heterotrophs) and ciliates during the Lagrangian survey over the mudflat,  
393 where resuspension occurred. In contrast, mixing (typically leading to dilution) with offshore  
394 waters was observed at the Eulerian site, except for free viruses and free bacteria at the  
395 bottom (gain), ANF (gain) and *Synechococcus* and ciliates (loss). No significant change was  
396 detected in autotroph biomass in any of the surveys (Fig. 7a) or in heterotroph biomass during  
397 the Lagrangian survey (Fig. 7b). In contrast, heterotroph biomass was decreased by 50% at  
398 the end of the Eulerian survey as expected from dilution with less heterotrophic offshore  
399 waters (Fig. 7b). Regardless, heterotroph biomass remained greater than autotroph biomass  
400 throughout both surveys.

401

#### 402 **4. Discussion**

403 In the present study, we aimed at testing in situ whether and how the pelagic system  
404 structure was modified during the rising tide by physical transfer of autotrophic and  
405 heterotrophic microorganisms. Physical transfer included mixing with offshore waters and  
406 sediment erosion and was evidenced by temporal changes in particulate inorganic matter  
407 concentration.

##### 408 *4.1 Decrease of resuspended microorganisms by grazing predators*

409 Over the mudflat, significant sediment erosion occurred under wave action, but at  
410 different rates across the intertidal area. These changes were reflected by subsequent changes  
411 in erodibility across the mudflat as bed friction velocity was kept constant during the  
412 Lagrangian survey. A very low erosion rate in the middle region of the Brouage mudflat with  
413 large bed friction velocities was indicative of low erodibility of the consolidated sediment,  
414 possibly due to desiccation during tidal emersion (Anderson and Howell 1984; Paterson et al.  
415 1990). On July 24, water content in the upper layer of mud fell from 55 to 46% during the 4 h  
416 low tide. Such periods of desiccation occurred on many days throughout the particularly dry,

417 windy and hot month of July 2008 (Dupuy et al., personal communication). Variability in  
418 erosion rates across the mudflat may also be attributed to changes in bioturbation intensity  
419 (Widdows et al. 1998). Specifically, more active bioturbators in the Brouage mudflat, such as  
420 *Scorbicularia plana* (Orvain 2005), are generally more abundant in the upper mudflat  
421 (Sauriau et al. 1989; Bocher et al. 2007; Orvain et al. 2007). Moreover, erodibility increase  
422 due to bioturbation activity should also be enhanced by low tide duration: the upper in the  
423 mudflat, the longer the low tide and hence, the higher the bioturbation pressure. Surprisingly,  
424 the input of taxon that are generally abundant in the sediment, such as diatoms, bacteria and  
425 nanoflagellates (Paterson et al. 2009), was not observed during sediment erosion. Differences  
426 in resuspension thresholds for benthic microorganisms may have been due to cell size,  
427 specific gravity, behaviour, or association with particles (Shimeta et al. 2002). However, bed  
428 friction velocities reaching an average of  $3.2 \text{ cm s}^{-1}$  due to waves prevented sedimentation of  
429 particles with settling velocities less than  $4 \text{ cm s}^{-1}$  (i.e. particles with diameters smaller than  
430  $320 \text{ }\mu\text{m}$ ) (Fredsoe and Deigaard 1992). Thus, considering the much lower density of organic  
431 matter compared to sedimentary matter and suspension thresholds determined by Shimeta et  
432 al. (2002), suspension thresholds were reached for all microorganisms included in the present  
433 study. Moreover, wave vertical velocities were undoubtedly greater than the swimming speed  
434 of any of these microorganisms ( $<1 \text{ mm s}^{-1}$ , Bauerfeind et al. 1986), precluding any migration  
435 process. In addition, all microorganisms counted in the present study were found at high  
436 densities in the Brouage muddy sediment before the rising tide, except for ciliates. As such, a  
437 significant increase in microorganism concentrations was expected to occur along with  
438 erosion of the muddy bed. Conversely, a stagnation or a decrease in the concentration of any  
439 microorganism during the Lagrangian survey therefore most likely indicated consumption by  
440 grazers.

441 Guarini et al. (2008) developed a model that simulates the dynamics of microalgal  
442 biomass in semi-enclosed littoral ecosystems and suggested that resuspension of the MPB

443 occurs at the beginning of the rising tide, even in the absence of simultaneous sediment  
444 erosion. Such recurrent MPB resuspension is consistent with the high proportion of benthic  
445 diatom species observed at the beginning of both surveys in the present study. Meanwhile,  
446 enrichment in benthic diatoms species was not significant in our survey. However, benthic  
447 diatom concentration simultaneously increased with mud erosion in the lower and upper part  
448 of the mudflat. Of the smaller autotrophs, only ANF significantly increased in the lower part  
449 of the mudflat, where sediment erosion was greatest, during the first hour of the Lagrangian  
450 survey. This significant increase in ANF concentration in the water column suggests that ANF  
451 concentrations in eroded sediment during the survey was at least  $10^6$  cell mL<sup>-1</sup>, which is a  
452 hundred times greater than previously reported average values in the first top cm of the BMO  
453 sediment ( $10^4$  cell mL<sup>-1</sup>, C. Dupuy personal communication). Yet, ANF most probably  
454 accumulated at the very surface of sediment in a layer of 1-2 cells thickness, just like diatoms  
455 does, to photosynthesize (Guarini et al., 2000). These findings support routine measurement  
456 of the detailed vertical distribution of microorganisms for estimation of erosion fluxes.  
457 *Synechococcus* concentrations remained low, and picophytoeukaryote concentration  
458 decreased during the same period. We therefore suggest that the erosion flux of benthic  
459 diatoms and ANF, largely present at the mud surface, was immediately overwhelmed by a  
460 grazing flux due to heterotrophic protists (HNF, ciliates), micrometazoan and mesometazoans  
461 planktonic organisms (Sherr et al. 1986; Leakey et al. 1992; Calbet et al. 2008) or benthic  
462 suspension feeders (Hughes 1969; Carlson et al. 1984).

463 Free virus concentration decreased during the Lagrangian survey, while it was expected  
464 to increase with resuspension as these microorganisms are also largely present in mud ( $10^{10}$   
465 cell mL<sup>-1</sup> sediment; Hewson et al. 2001, and the present study). Again, this suggests that virus  
466 resuspension flux during the rising tide due to waves was compensated by a loss process.  
467 However, adsorption of free viruses onto clay particles may also occur in addition to or as an  
468 alternative to grazing (Malits and Weinbauer 2009). Reversible sorption and hydrophobic

469 effects are linked to the ionic strength of the given environment, most notably to the  
470 concentration of cations like  $\text{Na}^+$ , which may change between bed sediment and water (Gerba  
471 1984). Finally, water agitation has been recently shown to enhance viral sorption to clay  
472 (Syngouna and Chrysikopoulos 2010). Therefore, together with wave agitation, availability of  
473 sorption sites on the clayed mud of the BMO (Helton et al. 2006), salt water may favour virus  
474 adsorption onto sedimentary particles. Similar to viruses, electrostatic properties, pH,  
475 temperature, and salinity are thought to govern the sorption of bacterial cells onto clay  
476 minerals (Jiang et al. 2007). As such, bacteria adsorption onto resuspended sedimentary  
477 particles should not be excluded during the Lagrangian survey. Free bacteria concentration  
478 remained constant while an increase was expected as these organisms are abundant in the mud  
479 ( $5.10^8$  cell  $\text{mL}^{-1}$ , Garet 1996 and  $10^9$  cell  $\text{mL}^{-1}$  in the present study) and were undoubtedly  
480 resuspended. However, no significant enrichment in attached bacteria was observed during  
481 the Lagrangian survey despite that a thousand-fold enrichment was expected from the large  
482 PIM increase (ten-fold) and the high concentration of bacteria in bed sediment ( $10^9$  cell  $\text{mL}^{-1}$ )  
483 compared to water ( $10^6$  cell  $\text{mL}^{-1}$ ). As free virus concentration did not strongly increase,  
484 significant enhancement of virally mediated bacterial mortality was unlikely. Thus, attached  
485 and free bacteria were most likely heavily grazed immediately after resuspension during the  
486 Lagrangian survey.

487         Significant HNF concentration increase during the Lagrangian survey is consistent with  
488 expected resuspension of benthic HNF given the bed friction velocities (due to waves) that  
489 largely exceeded thresholds for HNF resuspension (Shimeta et al. 2002;  $0.25\text{-}0.80$   $\text{cm s}^{-1}$ ). In  
490 contrast, HNF production (secondary production) could not explain concentration doubling,  
491 given nanoplankton growth rate ranging from 7 h (Dupuy et al, 2007) to 20 h (Calbet et al.  
492 2008; Liu et al. 2009). Thus, doubling of HNF concentration in the water column suggest that  
493 HNF concentration in eroded sediment during the survey was roughly  $10^5$  cell  $\text{mL}^{-1}$ , which is  
494 a hundred times greater than previously reported average values found in the first top cm of

495 the BMO sediment ( $10^3$  cell mL<sup>-1</sup>, C. Dupuy personal communication). This result suggests  
496 that HNF accumulated at the very surface of sediment during the present study and pinpoints  
497 again the importance of accounting for vertical distribution of microorganisms when  
498 estimating erosion fluxes. Similar zonation of nanoflagellates at the surface of sediment  
499 compared to deeper layers have been previously reported during summer periods in the North  
500 Sea (Hondeveld et al. 1994) and also in the BMO in July 2008 (Dupuy et al., submitted). In  
501 any case, after 2 h, the decrease in HNF concentration during the Lagrangian survey indicated  
502 grazing on HNF by ciliates or micrometazoan and mesometazoan planktonic organisms  
503 (Sherr et al. 1986; Hartmann et al. 1993; Calbet et al. 2008) also buffered resuspension flux.

504 In contrast, a significant increase in ciliate concentration during the Lagrangian survey  
505 could not be attributed to benthic transfer that accompanies mud erosion. Although some  
506 ciliate genera can be found in sediment, such as scuticociliates (*Uronema* sp.), ciliate  
507 concentration is generally very low in mud sediments (Giere 1993), with concentrations lower  
508 than 20 cell mL<sup>-1</sup> in the BMO surficial sediment (C. Dupuy, personal communication).  
509 Simulated erosion of sediment cores taken in the BMO during the same period as the present  
510 study confirmed ciliates erosion was insignificant (C. Dupuy, personal communication).  
511 Besides, ciliates taxa found in the present study were Order Oligotrichida (*Strombidium* spp.)  
512 and Order Tintinnida (*Tintinnopsis* spp.), which are generally part of the suprabenthos due to  
513 behavioural adaptations leading to depth zonation above the sediment-water interface after  
514 vertical migration when vertical flow motion is small. Compared to other groups of  
515 microorganisms analysed in the present study, ciliates are relatively more motile organisms  
516 (velocities up to 0.5 mm s<sup>-1</sup>) that can control their position in the water column at low  
517 turbulence levels (Jonsson 1989). Ciliate concentration increase during the Lagrangian survey  
518 may be attributed to redistribution by waves vertical stirring of ciliates accumulated at a  
519 particular depth during slack tide.

520

521 *4.2 Mixing with offshore waters*

522         Mixing (dilution or enrichment) with offshore waters was expected during the Eulerian  
523 survey, where water depth varied. It should be noted that the 80% confidence interval around  
524 prediction from mixing with offshore waters reduces when offshore waters are less  
525 concentrated than inner basin waters (heterotrophic microorganisms) while it is reversed when  
526 offshore are more concentrated than inner basin waters (autotrophic microorganisms). Thus,  
527 detecting deviation from dilution prediction should be more accurate than detecting deviation  
528 from import prediction.

529         The PIM concentration evolved as predicted by dilution during the Eulerian survey,  
530 indicating that no significant erosion or sedimentation occurred. Thus, settling velocity of  
531 suspended particles should be comparable to mean wave bed friction velocities, ranging from  
532 1.4 to 0.5 cm s<sup>-1</sup>, while bed sediment erosion threshold should be larger than 1.4 cm s<sup>-1</sup>. In  
533 contrast, during the Lagrangian survey, a strong increase in PIM concentration indicated that  
534 bed friction velocities were high enough to erode the mud. Bed friction velocity due to the  
535 tidal current (1.3 cm s<sup>-1</sup>) was lower than the largest bed friction velocity observed during the  
536 Eulerian survey which did not cause significant erosion. Thus, mud erosion during the  
537 Lagrangian survey was more likely driven by bed friction velocities due to waves (average  
538 velocity of 3.2 cm s<sup>-1</sup> and 4.5 cm s<sup>-1</sup> maximum) as suggested by Bassoullet et al. (2000).  
539 However, the current study only indicates that the erosion threshold for the fine-grained mud  
540 sediment of the Brouage mudflat (median grain size was 10 to 12 µm) lies between 1.4 cm s<sup>-1</sup>  
541 (largest value during Eulerian survey during which erosion was not observed) and 4.5 cm s<sup>-1</sup>  
542 (largest value during Lagrangian survey during which erosion was observed) in terms of bed  
543 friction velocity.

544

545         During the Eulerian survey, no significant change in diatom concentration was detected  
546 reflecting similar order of magnitude of concentration in the inner basin and in the north of

547 the basin. However, a total community change occurred with replacement of benthic diatoms  
548 by pelagic diatoms in proportion of water depth change during the rising tide. No significant  
549 primary production of diatoms was expected given the short duration of the Eulerian survey  
550 compared to the generation time for microphytoplankton (1 division  $d^{-1}$ , Calbet and Landry  
551 2004 to 2 divisions  $d^{-1}$ , Dupuy et al. 2007) and water turbidity (Struski and Bacher 2006;  
552 Bouman et al. 2010). Thus, mixing was the most likely dominant process.

553         Significantly lower than expected concentrations (based on mixing with offshore  
554 waters) of low motility *Synechococcus* (at the surface and at the bottom) suggest that grazing  
555 pressure was strong during tidal flow due to microzooplankton, mesozooplankton and/or  
556 bivalve mollusks (*Macoma balthica*, *Scrobicularia plana*) (Hugues 1969; Hartmann et al.  
557 1993; Dupuy et al. 1999). Ciliates also exhibited lower than expected concentrations at the  
558 bottom. However, for these motile organisms, the assumption of a vertically homogeneous  
559 distribution was probably no longer true as turbulence intensity decayed during the Eulerian  
560 survey. Thus, ciliates losses may not be attributed to grazing only. Motility may also explain  
561 the opposite dynamics of nanoflagellates during the Eulerian survey between surface and  
562 bottom, given their swimming speed can reach 0.3 to 0.5  $mm\ s^{-1}$  and yield a transport of 1 to 2  
563 m after one hour (Bauerfeind et al. 1986). However, an overall significant increase in ANF  
564 concentration at the end of the Eulerian survey suggested that primary production started.

565         Conversely, during the first portion of the Eulerian survey, free virus and free bacteria  
566 concentration significantly increased at the surface compared to the offshore water dilution  
567 curve, suggesting that secondary production or desorption dominated over grazing. This  
568 synchronous increase was congruent with the synchronous virus and bacteria dynamics  
569 usually observed in BMO at the monthly scale in summer (Ory et al. 2010, 2011).

570

571         4.3 Strengths and limitations of the sampling strategy

572 Adapting sampling strategy to disentangle mixing with offshore waters and  
573 resuspension and separating physical processes from biotic processes using PIM as a  
574 reference lead to the conclusion that grazing pressure must be intense during rising tide.  
575 However, temporal changes in concentrations that follow the dilution curve in an Eulerian  
576 survey or remain constant in a Lagrangian survey simply mean that loss and gain processes  
577 balance each other out. In addition, conclusive demonstration of loss or gain processes  
578 requires that temporal changes in surveys are larger than uncertainties on initial conditions. In  
579 the present study, uncertainties in PIM, diatoms, picoeukaryotes and attached bacteria  
580 concentrations at the beginning of surveys reached 100%, which prevented the detection of  
581 any significant decrease. Yet, significant increases could be detected when values more than  
582 doubled, as seen for PIM. These large uncertainties have different origins. For PIM,  
583 uncertainties were mainly due to large differences between the Lagrangian and Eulerian  
584 samples taken when surveys started and advocate for increasing sampling effort and  
585 localization precision in the intertidal area where large horizontal spatial gradients may exist.  
586 For diatoms, attached bacteria and picoeukaryotes, large uncertainties also came from large  
587 difference between the Eulerian samples and points out the low precision on concentration  
588 determination for some microorganisms. Reducing these uncertainties requires increased  
589 sample volume and superior enumeration efforts.

590

## 591 **5. Conclusions**

592 During a rising tide, expected water column enrichment of benthic microorganisms  
593 (small to large autotrophs and heterotrophs) from sediment resuspension was largely  
594 overwhelmed by loss processes, except for nanoflagellates (ANF and HNF). The dominant  
595 loss process was likely grazing. However, adsorption onto clayed particles may have also  
596 masked enrichment for free viruses and bacteria . A combination of resuspension and  
597 grazing/adsorption processes led to non-significant changes in both heterotroph and autotroph



598 total biomass during the rising tide in the nearshore area. In the meanwhile, offshore waters  
599 imported autotrophic organisms, mainly *Synechococcus*, while heterotrophic microorganisms  
600 were diluted. However, autotrophic organisms import was significantly grazed. As a result,  
601 combination of offshore waters import and grazing led to stability of autotrophs biomass in  
602 the deeper areas of the BMO, while heterotrophs biomass was reduced by 50%. Lastly, when  
603 resuspension occurred over a tidal flat during a rising tide, the water column evolved to a less  
604 heterotrophic structure over the mudflat in the deepest part of the semi-enclosed bay  
605 compared to nearshore. Thus, the present study suggests that this differential evolution mainly  
606 reflects dilution with low concentrated offshore waters, as grazing pressure erased any  
607 microorganisms inputs accompanying physical transfers due to bed erosion or offshore waters  
608 mixing.

609

## 610 **Acknowledgments**

611 The work was supported by the French ANR (Agence Nationale pour la Recherche)  
612 through the VASIREMI project “Trophic significance of microbial biofilms in tidal flats”  
613 (grant no. ANR-06-BLAN-0393-01). We are grateful to Martine Bréret, Camille Fontaine,  
614 Françoise Mornet and the personnel at both RV Tidalou and Estran for their technical support.  
615 We thank Pierre Richard for the Lagrangian buoys. We are also grateful to Carolyn Engel-  
616 Gautier and Proof-reading-service.com Ltd for English corrections.

617

618

619

620

621

622

623

624 **References**

625

626 Alongi, D. M. 1991. Flagellates of benthic communities: characteristics and methods of study,  
627 p. 57–75. In D. J. Patterson [ed.], *The Biology of Free-living Heterotrophic Flagellates*.  
628 Clarendon Press, Oxford.

629 Aminot, A., and M. Chaussepied. 1983. *Manuel des analyses chimiques en milieu marin*.  
630 CNEXO, Brest.

631 Anderson, F. E., and B. A. Howell. 1984. Dewatering of an unvegetated muddy tidal flat  
632 during exposure – dessication or drainage? *Estuaries* **7**: 225-232.

633 Bassoulet, P., P. Le Hir, D. Gouleau, and S. Robert. 2000. Sediment transport over an  
634 intertidal mudflat: field investigations and estimation of fluxes within the `Baie de  
635 Marennes-Oleron (France). *Cont. Shelf Res.* **20**: 1635-1653.

636 Bauerfeind, E., Elbrächter, M., Steiner, R. and J. Thronen. 1986. Application of Laser  
637 Doppler Spectroscopy (LDS) in determining swimming velocities of motile  
638 phytoplankton. *Mar Biol* **93**: 323-327.

639 Blanchard, G.F, and V. Cariou-Le Gall. 1994. Photosynthetic characteristics of  
640 microphytobenthos in Marennes-Oleron Bay, France : Preliminary results. *J. Exp. Mar.*  
641 *Biol. Ecol.* **182**: 1–14.

642 Blanchard, G.F., J. M. Guarini, P. Richard, and P. Gros. 1997. Seasonal effect on the  
643 relationship between the photosynthetic capacity of intertidal microphytobenthos and  
644 short-term temperature changes. *J. Phycol.* **33**: 723-728.

645 Blanchot, J., and M. Rodier. 1996. Picophytoplankton abundance and biomass in the western  
646 tropical Pacific Ocean during the 1992 El Nino year: results from flow cytometry. *Deep*  
647 *Sea Res Part I: Oceanogr. Res. Papers* **43**: 877-895.

648 Bocher, P., T. Piersma, A. Dekinga, C. Kraan, M. G. Yates, T. Guyot, E. O. Folmer, and G.  
649 Radenac. 2007. Site- and species-specific distribution patterns of mollusks at five

650 intertidal soft-sediment areas in northwest Europe during a single winter. *Mar. Biol.*  
651 **151**:577-594.

652 Bouman, H. A. , T. Nakane, K. Oka, K. Nakata, K. Kurita, S. Sathyendranath, and T. Platt.  
653 2010. Environmental controls on phytoplankton production in coastal ecosystems: A  
654 case study from Tokyo Bay. *Est. Coast. Shelf. Sci.* **87**: 63-72.

655 Calbet, A., and M. R. Landry. 2004. Phytoplankton growth, microzooplankton grazing, and  
656 carbon cycling in marine systems. *Limnol. Oceanogr.* **49**:51-57.

657 Calbet, A., I. Trepas, R. Almeda, V. Saló, E. Saiz, J. I. Movilla, M. Alcaraz, L. Yebra, and R.  
658 Simó. 2008. Impact of micro- and nanograzers on phytoplankton assessed by standard  
659 and size-fractionated dilution grazing experiments. *Aquat. Microb. Ecol.* **50**: 145-156.

660 Cammen, L.M. 1991. Annual bacterial production in relation to benthic microalgal production  
661 and sediment oxygen uptake in an intertidal sandflat and an intertidal mudflat. *Mar.*  
662 *Ecol. Prog. Ser.* **71**: 13-25.

663 Caron, D. A. 1983. Technique for enumeration of heterotrophic and phototrophic  
664 nanoplankton, using epifluorescence microscopy, and comparison with other  
665 procedures. *Appl. Environ. Microbiol.* **46**: 491-498.

666 Carlson, D. Townsend, D. W., Hilyard, A. L., Eaton J. F. 1984. Effect of an Intertidal Mudflat  
667 on Plankton of the Overlying Water column. *Can. J. Fish. Aquat. Sci.*, 41, 1523-1528.

668 Danovaro, R., C. Corinadelsi, M. Filippini, U. R. Fisher, M. O. Gessner, S. Jacquet, M.  
669 Magagnini, and B. Velimirov. 2008. Viriobenthos in freshwater and marine sediments:  
670 a review. *Fresh. Biol.* **53**: 1186-1213.

671 Dupuy, C., S. Le Gall, H. J. Hartmann, and M. Bréret. 1999. Retention of ciliates and  
672 flagellates by the oyster *Crassostrea gigas* in French Atlantic coastal ponds: protists as  
673 a trophic link between bacterioplankton and benthic suspension-feeders. *Mar. Ecol.*  
674 *Prog. Ser.* **177**: 165-175.

- 675 Dupuy, C., A. Pastoureaud, M. Ryckaert, P. G. Sauriau, and H. Montanié. 2000. Impact of the  
676 oyster *Crassostrea gigas* on the microbial community in Atlantic coastal ponds near La  
677 Rochelle. *Aquat. Microb. Ecol.* **22**: 227-242.
- 678 Dupuy, C., M. Ryckaert, S. Le Gall, and H. J. Hartmann. 2007. Seasonal variations of  
679 planktonic communities in Atlantic Coastal pond: importance of nanoflagellates.  
680 *Microb. Ecol.* **53**: 537-548.
- 681 Epstein, S. S. 1997. Microbial food webs in marine sediments. I. Trophic interactions and  
682 grazing rates in two tidal flat communities. *Microb. Ecol.* **34**:188-198.
- 683 Fenchel, T. 1969. The ecology of marine microbenthos. IV. Structure and function of the  
684 benthic ecosystem, its chemical and physical factors and the microfauna communities  
685 with special reference to the ciliated protozoa. *Ophelia* **5**:1-182.
- 686 Fredsoe, J., and R. Deigaard. 1992. Mechanics of coastal sediment transport. 369 p. In World  
687 Scientific [ed.], *Advanced Series on Ocean Engineering* 3.
- 688 French, J.R., H. Burningham, and T. Benson. 2008. Tidal and Meteorological Forcing of  
689 Suspended Sediment Flux in a Muddy Mesotidal Estuary. *Estuaries Coasts* **31** : 843-  
690 859.
- 691 Fournier, J., Dupuy, C., Bouvy, B., Courrodon-Real, M., Charpy, L., Pouvreau, S., Le  
692 Moullac, G., Le Penec, M., Cochard, J.C. 2012 Pearl oysters *Pinctada margaritifera*  
693 grazing on natural plankton in Ahe atoll lagoon (Tuamotu archipelago, French  
694 Polynesia). *Marine Pollution Bulletin* **65** : 490-499
- 695 Garet, M. J. 1996. Transformation bactérienne de la matière organique dans les sédiments  
696 côtiers. Relation entre les métabolismes respiratoires et les activités exoprotéolytiques  
697 bactériennes, PhD Microbiologie : Univ. Bordeaux 2.
- 698 Garstecki, T., S. A. Wickham, and H. Arndt. 2002. Effects of experimental sediment resus-  
699 pension on a coastal planktonic microbial food web. *Est. Coast. Shelf. Sci.* **55**: 751-762.

- 700 Gasol, J. M. 1993. Benthic flagellates and ciliates in fine freshwater sediments: calibration of  
701 a live counting procedure and estimation of their abundances. *Microb. Ecol.* **25**:247-  
702 262.
- 703 Gerba, C. P. 1984. Applied and theoretical aspects of virus adsorption to surfaces, 30: 133-  
704 168. In *Advances in Applied microbiology* [ed.], Academic press, Inc.
- 705 Giere, O. 1993. *Meiobenthology. The microscopic fauna in aquatic sediments*, 328 pp.  
706 Springer-Verlag, Berlin.
- 707 Grémare, A., Amouroux, J.M., Cauwet, G., Charles, F., Courties, C., deBovée, F., Dinet, A.,  
708 Devenon, J.L., Durrieu de Madron, X., Ferré, B., Fraunié, P., Joux, F., Lantoiné, F.,  
709 Lebaron, P., Naudin, J.J., Palanques, A., Pujo-Pay, M., Zudaire, L. 2003. The effects of  
710 a strong winter storm on physical and biological variables at a shelf site in the  
711 Mediterranean. *Oceanologica Acta*, 26(4), 407-419.
- 712 Guarini, J. M., Blanchard, G.F., Gros, Ph., Gouleau, D., Bacher, C. 2000. Dynamic model of  
713 the short-term variability of microphytobenthic biomass on temperate intertidal  
714 mudflats. *Mar. Ecol. Prog. Ser.* **195**: 291-303.
- 715 Guarini, J. M., N. Sari, and C. Moritz. 2008. Modelling the dynamics of the microalgal  
716 biomass in semi-enclosed shallow-water ecosystems. *Ecol. Modeling* **211**: 267-278.
- 717 Guizien, K., F. Charles, D. Hurther, and H. Michallet. 2010. Spatial redistribution of *Ditrupa*  
718 *arietina* (soft bottom Mediterranean epifauna) during a moderate swell event: evidence  
719 and implications for biotic quality indices. *Cont. Shelf Res.* **30**: 239-251.
- 720 Guizien, K., and A. Temperville. 1999. Frottement de fond sous une houle irrégulière. *C. R.*  
721 *Acad. Sci. Paris*, t. 327, Série Iib: 1375-1378.
- 722 Haas, L.W. 1982. Improved epifluorescence microscopy for observing planktonic  
723 microorganisms. *Ann. Inst. Oceanogr.* **58**: 261-266.

- 724 Hartmann, H. J., H. Taleb, L. Aleya, and N. Lair. 1993. Predation on ciliates by the  
725 suspension-feeding calanoid copepod *Acanthodiaptornus denticornis*. Can. J. Fish.  
726 Aquat. Sci. Paris. **50**:1382-1393.
- 727 Hervouet, J. M., and L. Van Haren. 1994. TELEMAC-2D Principle Note (Electricité de  
728 France, Technical Report HE- 43/94/051/B).
- 729 Hervouet, J. M. 2007. Hydrodynamics of Free Surface Flows: Modelling With the Finite  
730 Element Method, Wiley-Blackwell, 360 pp.
- 731 Hewson, I., J. M. O'Neil, C. Heil, G. Bratbak, and D. Dennison. 2001. Effects of concentrated  
732 viral communities on photosynthesis and community composition of co-occurring  
733 benthic microalgae and phytoplankton. Aquat. Microb. Ecol. **25**: 1-10.
- 734 Herlory, O., J. M. Guarini, P. Richard, and J. F. Blanchard. 2004. Microstructure of  
735 microphytobenthic biofilm and its spatio-temporal dynamics in an intertidal mudflat  
736 (Aiguillon Bay, France). Mar. Ecol. Prog. Ser. **282**: 33-44.
- 737 Hondeveld B.J.M., Nieuwland G., van Duyl F.C., Bak R.P.M. 1994. Temporal and spatial  
738 variations in heterotrophic nanoflagellate abundance in North Sea sediment. Mar. Ecol.  
739 Prog. Ser. **109**: 235-243.
- 740 Hughes, R.N. 1969. A study of feeding in *Scrobicularia plana*. J. Mar. Biol. Ass. U. K. **49**:  
741 805-823.
- 742 Jiang, D., Q. Huang, P. Cai, X. Rong, and W. Chen. 2007. Adsorption of *Pseudomonas*  
743 *putida* on clay minerals and iron oxide. Colloids and surfacesB : Biointerfaces **54**: 217-  
744 221.
- 745 Jonsson P.R. 1989. Vertical distribution of planktonic ciliates – an experimental ciliates : an  
746 experimental analysis of swimming behaviour. Mar. Ecol. Prog. Ser. **52**: 39-53.
- 747 Kemp, P. F. 1988. Bacterivory by benthic ciliates: significance as a carbon source and impact  
748 on sediment bacteria. Mar. Ecol. Prog. Ser. **49**:163-169.

- 749 Koroleff, F., 1969. Direct determination of ammonia as indophenol blue. International  
750 Council for the Exploration of the Sea, 1969/C:9, Hydrol Commun, pp 19-22.
- 751 Labry, C., A. Herbland, and D. Delmas. 2002. The role of phosphorus on planktonic  
752 production of the Gironde plume waters in the Bay of Biscay. *J. of Plankton Res.* **24**:  
753 97-117.
- 754 Leakey, R. J. G., P. H. Burlull, and M. A. Sleight. 1992. Planktonic ciliates in Southampton  
755 Water: abundance, biomass, production, and role of pelagic carbon flow. *Mar. Biol.* **14**:  
756 67-83.
- 757 Liu, H., K. Suzuki, J. Nishioka, R. Sohrin, and T. Nakatsuka. 2009. Phytoplankton growth  
758 and microzooplankton grazing in the Sea of Okhotsk during late summer of 2006.  
759 *Deep-Sea Res. I.* **56**: 561-570.
- 760 Lucas, C.H., J. Widdows, M. D. Brinsley, P. N. Salkeld, and P. M. J. Herman. 2000. Benthic-  
761 pelagic exchange of microalgae at a tidal flat. 1. Pigment analysis. *Mar. Ecol. Prog. Ser.*  
762 **196**: 59-73.
- 763 Malits, A., and M. G. Weinbauer. 2009. Effect of turbulence and viruses on prokaryotic cell  
764 size, production and diversity. *Aquat. Microb. Ecol.* **54**: 243-254.
- 765 Marie, D., F. Partensky, N. Simon, L. Guillou, and D. Vaultot. 2000. Flow cytometry analysis  
766 of marine picoplankton. In: Diamond RA, DeMaggio S [ed.], *In living color. Protocols*  
767 *in flow cytometry and cell sorting.* Springer-Verlag, Berlin.
- 768 Marquis, E., N. Niquil, D. Delmas, H. J. Hartmann, D. Bonnet, F. Carlotti, A. Herbland, C.  
769 Labry, B. Sautour, P. Laborde, and C. Dupuy. 2007. Planktonic food web dynamics  
770 related to phytoplankton bloom development on the continental shelf of the Bay of  
771 Biscay, French coast. *Est. Coast. Shelf. Sci.* **73**: 223-235.
- 772 Mehta, J.A., E. J. Hayter, W. R. Parker, R. B. Krone, and A. M. Teeter. 1989. Cohesive  
773 sediment transport. I. Process description. *J. Hydraulic Eng.* **115**:1076-1093.

- 774 Nezan, E., 1996. Surveillance du Phytoplankton marin : manuel illustré adapté à la formation  
775 des analystes. (IFREMER, Eds.). Brest.
- 776 Nicolle, A., and M. Karpytchev. 2007. Evidence for spatially variable friction from tidal  
777 amplification and asymmetry in the Pertuis Breton (France). Cont. Shelf Res. **27**: 2346-  
778 2356.
- 779 Noble, R.T., and J. A. Fuhrman. 1998. Use of SYBR Green I for rapid epifluorescence counts  
780 of marine viruses and bacteria. Aquat. Microb. Ecol. **14**: 113-118.
- 781 Orvain, F. 2005. A model of sediment transport under the influence of bioturbation activities:  
782 generalisation to a key-species *Scrobicularia plana*. Mar. Ecol. Progr. Ser. **286**: 43-56.
- 783 Orvain F., P. G. Sauriau, A. Sygut, L. Joassard, and P. Le Hir. 2004. Roles of *Hydrobia ulvae*  
784 bioturbation and the physiological stage of microphytobenthic mats in resuspended  
785 sediment and pigment fluxes. Mar. Ecol. Prog. Ser. **278**: 205-223.
- 786 Ory, P., H. J. Hartmann, F. Jude, C. Dupuy, Y. Del Amo, P. Catala, F. Mornet, V. Huet, B.  
787 Juan, D. Vincent, B. Sautour, and H. Montanié. 2010. Pelagic food web patterns: do  
788 they modulate virus and nanoflagellate effects on picoplankton during the  
789 phytoplankton spring bloom? Environ. Microbiol., **12** : 2755-2772
- 790 Ory, P., Palesse, S., Delmas ,D. and Montanié H., 2011 In situ structuring of virioplancton  
791 through bacterial exoenzymatic activity ; interaction with phytoplankton. Aquatic  
792 microbial ecology, **64**: 233-252.
- 793 Paterson, D.M., R. M. Crawford, and C. Little. 1990. Subaerial exposure and changes in the  
794 stability of intertidal estuarine sediments. Est. Coast. Shelf. Sci. **30**:541-556.
- 795 Paterson, D. M., R. Aspden, and K. S. Black. 2009. Intertidal flats: Ecosystem functioning of  
796 soft sediments systems. In: Perillo GME, Wolanski E, Cahoon DR, Brinson MM [ed.],  
797 Coastal Wetlands: An Integrated Ecosystem Approach. Elsevier.



- 798 Pelegri, S. P., J. R. Dolan, and F. Rassoulzadegan. 1999. Use of high temperature catalytic  
799 oxidation (HTCO) to measure carbon content of microorganisms. *Aquat. Microb. Ecol.*  
800 **16**: 273-280.
- 801 Pusceddu, A., C. Fiordelmondo, and R. Danovaro. 2005. Effects on the Benthic Microbial  
802 Loop in Experimental Microcosms. *Microb. Ecol.* **50**: 602-613.
- 803 Ricard, M., 1987. Atlas du phytoplancton marin, vol. 2. (CNRS, Eds.). Paris.
- 804 Schmidt, J. L., J. W. Deming, P. A. Jumars, and R. G. Keil. 1998. Constancy of bacterial  
805 abundance in surficial marine sediments. *Limnol. Oceanogr.* **43**: 976-982.
- 806 Seymour, J. R., L. Seuront, and J. G. Mitchell. 2007. Microscale gradients of planktonic  
807 microbial communities above the sediment surface in a mangrove estuary. *Est. Coast.*  
808 *Shelf. Sci.* **73**: 651-666
- 809 Sherr, E., B. F. Sherr, and G. A. Paffenhofer. 1986. Phagotrophic protozoa as food for  
810 metazoans: a "missing" trophic link in marine pelagic food webs? *Mar. Microb. Food*  
811 *Webs* **1**:61-80.
- 812 Sherr, E. B., D. A. Caron, and B. F. Sherr. 1994. Staining of heterotrophic protists for  
813 visualisation via epifluorescence microscopy. In: Kemp, PF, Sherr, BF, Sherr, EB, Cole,  
814 JJ [ed.], 213-227. *Handbook of Methods in Aquatic Microbial Ecology*. Lewis  
815 Publishers, Boca Raton, FL.
- 816 Shimeta, J., and J. Sisson. 1999. Taxon-specific tidal resuspension of protists into the subtidal  
817 benthic boundary layer of a coastal embayment. *Mar. Ecol. Prog. Ser.* **177**: 51-62.
- 818 Shimeta, J, C. L. Amos, S. E. Beaulieu, and O. M. Ashiru. 2002. Sequential resuspension of  
819 protists by accelerating tidal flow: Implications for community structure in the benthic  
820 boundary layer. *Limnol. Oceanogr.* **47**: 1152-1164.

- 821 Shimeta, J., C. L. Amos, S. E. Beaulieu, and S. L. Katz. 2003. Resuspension of benthic  
822 protists at subtidal coastal sites with differing sediment composition. *Mar. Ecol. Prog.*  
823 *Ser.* **259**: 103-115.
- 824 Sournia, A., 1986. *Atlas du phytoplancton marin*, vol. 1. (CNRS, Eds.). Paris.
- 825 Struski, C., and C. Bacher. 2006. Preliminary estimate of primary production by phytoplank-  
826 ton in Marennes-Oleron Bay, France. *Est. Coast. Shelf. Sci.* **66**: 323-334.
- 827 Syngouna, V.I. and Chrysikopoulos, C.V. 2010. Interaction between viruses and clays in stat-  
828 ic and dynamic bacth system. *Environ Sci Technol* 44: 4539-4544
- 829 Van Duyl, F.C., and A. J. Kop. 1994. Bacterial production in North Sea sediments: clues to  
830 seasonal and spatial variations. *Mar. Biol.* **235**: 323-327.
- 831 Widdows, J., M. D. Brinsley, and M. Elliott. 1998. Use of in situ flume to quantify particle  
832 flux. 139:85-97, In: Black K.S., Paterson D.M., Cramp A. [ed.], *Sedimentary processes*  
833 *in the Intertidal Zone*. Geol. Soc. London, Special publication.
- 834 Wu, Q. L., Y. Chen, K. Xu, Z. Liu, and M. W. Hahn. 2007. Intra-habitat heterogeneity of mi-  
835 crobial food web structure under the regime of eutrophication and sediment resuspen-  
836 sion in the large subtropical shallow Lake Taihu, China. *Hydrobiologia* **581**: 241-254.
- 837
- 838

Figure 1: Map of the Marennes-Oléron Bay in Europe. The grey area indicates land and the contour labeled 0 delimites the largest extent of the intertidal area (lowest sea level during the highest tidal coefficient). Open circles indicate the successive locations of the Lagrangian survey stations, the open square indicates the Eulerian survey location and the filled triangle indicates the ADV location. Trajectories simulated with the Telemac model are displayed: thin lines figure trajectories reaching the Eulerian survey location at 17:20 h (solid) and 18:40 h (dashed) and the thick line figures trajectory leaving the Eulerian survey location at 16:00 h.

Figure 2: Expected temporal changes in concentrations during a Lagrangian survey (black line) and during a Eulerian survey (gray line) of the water column.

Figure 3: (a) Wind speed at La Rochelle Aérodrome and significant wave height ( $H_s$ ) on the intertidal flat during high tide (light gray) on 24 July, 2008. (b) Measured bed friction velocities associated with the tidal current (open triangles) and computed bed friction velocities associated with waves in a constant 40 cm water depth during the Lagrangian survey (filled circles for the maximum, open circles for the average) and for water depth increasing from 1.1 to 3.1 m during the Eulerian survey (filled squares for the maximum, open squares for the average).

Figure 4: Temporal changes in concentration of particulate inorganic matter (PIM) in the middle of the water column during the Lagrangian survey (white bar) and during the Eulerian survey (square) at the surface (gray) and at the bottom (white) of the water column. The black vertical bar represents the average concentration in the middle of the water column in the lower part of the mudflat when surveys started with its 80% confidence interval. Lines display the 80% confidence interval of concentrations calculated assuming only mixing with

incoming offshore waters when tide rose during the Eulerian survey (see formula in the Methods section).

Figure 5: Temporal changes in the abundances of autotrophic organisms: benthic diatoms (a), pelagic diatoms (b), autotrophic nanoflagellates (ANF, c), Picophytoeukaryots (d) and *Synechococcus* (e) in the middle of the water column during the Lagrangian survey (white bar) and during the Eulerian survey (square) at the surface (gray) and at the bottom (white) of the water column. The black vertical bar represents the average concentration in the middle of the water column in the lower part of the mudflat when surveys started with its 80% confidence interval. Lines display the 80% confidence interval of concentrations calculated assuming only mixing with incoming offshore waters when tide rose during the Eulerian survey (see formula in the Methods section).

Figure 6: Temporal changes in the abundances of heterotrophic organisms: free viruses (a), free bacteria (b), attached bacteria (c), heterotrophic nanoflagellates (HNF, d) and ciliates (e) in the middle of the water column during the Lagrangian survey (white bar) and during the Eulerian survey (square) at the surface (gray) and at the bottom (white) of the water column. The black vertical bar represents the average concentration in the middle of the water column in the lower part of the mudflat when surveys started with its 80% confidence interval. Lines display the 80% confidence interval of concentrations calculated assuming only mixing with incoming offshore waters when tide rose during the Eulerian survey (see formula in the Methods section).

Figure 7: Temporal trends in the autotrophs (a) and heterotrophs (b) biomass in the middle of the water column during the Lagrangian survey (white bar) and during the Eulerian survey (square) at the surface (gray) and at the bottom (white) of the water column. The black

vertical bar represents the average concentration in the middle of the water column in the lower part of the mudflat when surveys started with its 80% confidence interval.

Table 1: Concentrations of parameters at the north station on July 12 and 29, 2008, used as offshore value  $C_{\text{ext}}$  in equation (1).

	July 12 / July 29
PIM	18.2 / 6.67 mg L <sup>-1</sup>
Pelagic diatoms	112.7 / 52.8 cell mL <sup>-1</sup>
Benthic diatoms	17.3 / 4.2 cell mL <sup>-1</sup>
ANF	1.8 / 1.0 10 <sup>3</sup> cell mL <sup>-1</sup>
Picoeukaryots	5.5 / 2.88 10 <sup>3</sup> cell mL <sup>-1</sup>
<i>Synechococcus</i> sp.	1.44 / 2.25 10 <sup>4</sup> cell mL <sup>-1</sup>
Free virus	3.8 / 2.34 10 <sup>6</sup> cell mL <sup>-1</sup>
Free bacteria	2.65 / 2.48 10 <sup>6</sup> cell mL <sup>-1</sup>
Attached bacteria	5.3 / 7.5 10 <sup>3</sup> cell mL <sup>-1</sup>
HNF	1.5 / 0.6 10 <sup>3</sup> cell mL <sup>-1</sup>
Ciliates	3.66 / 4.58 cell mL <sup>-1</sup>

Table 2: Conversion factors and their corresponding literature reference used to convert abundance to biomass of carbon for each type of plankton organism.

<b>Cells or organism</b>	<b>Conversion factor (pg C/cell)</b>	<b>Reference</b>
Bacteria	0.016	Labry et al. (2002)
Synechococcus	0.104	Blanchot and Rodier (1996)
Picoeukaryotes	0.104	Blanchot and Rodier (1996)
Nanoflagellates	3.14	Pelegri et al. (1999)
Ciliates	3.14	Pelegri et al. (1999)
Diatoms	225	Fournier et al. (2012)

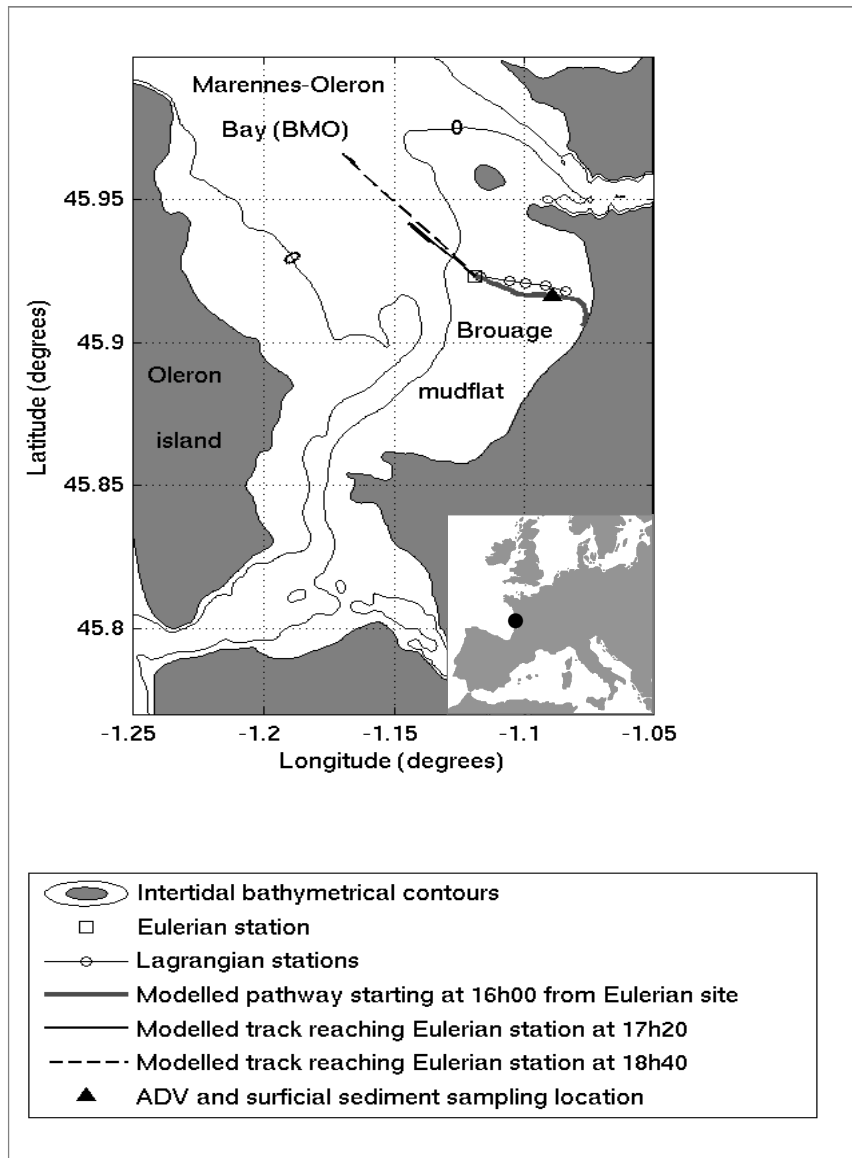


Figure 1



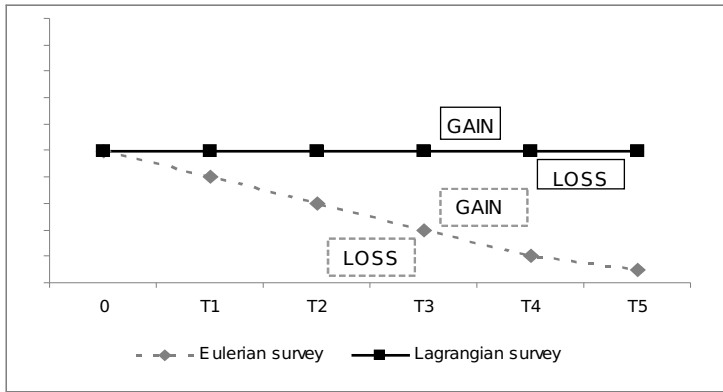


Figure 2

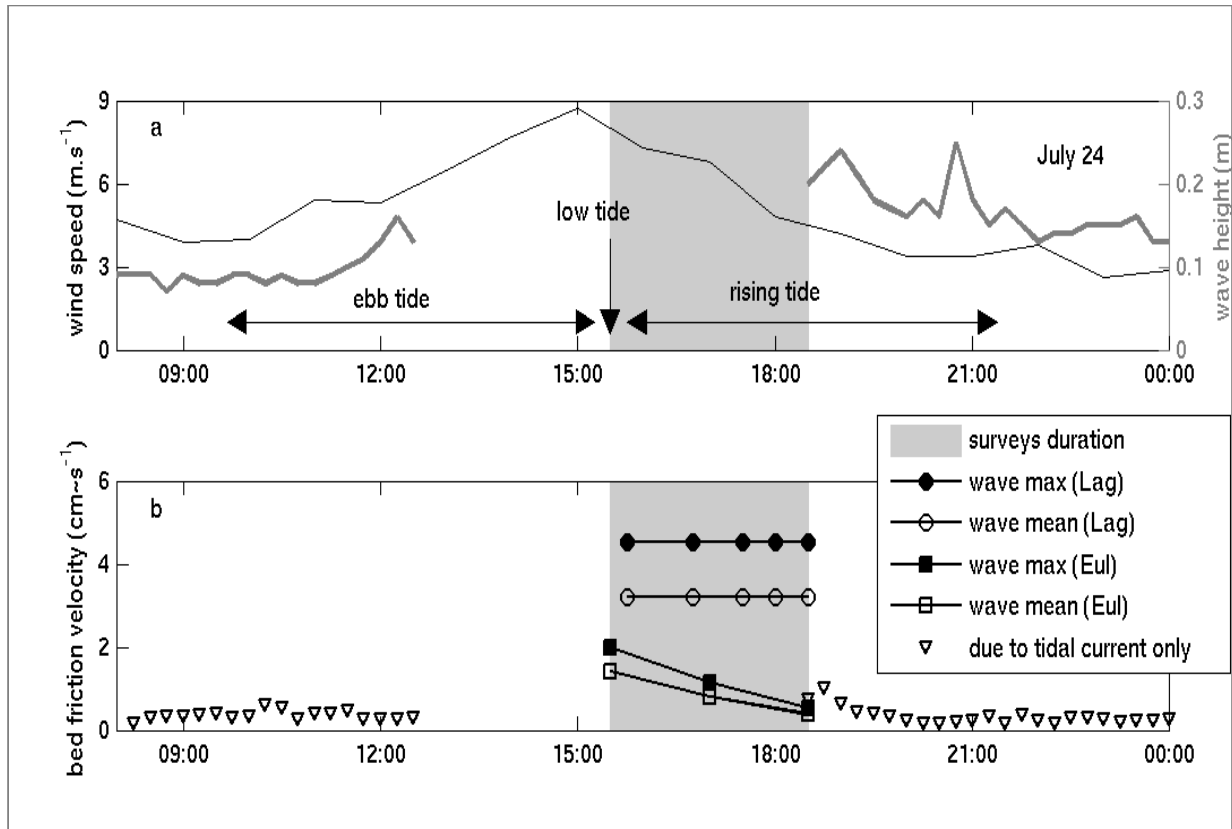


Figure 3

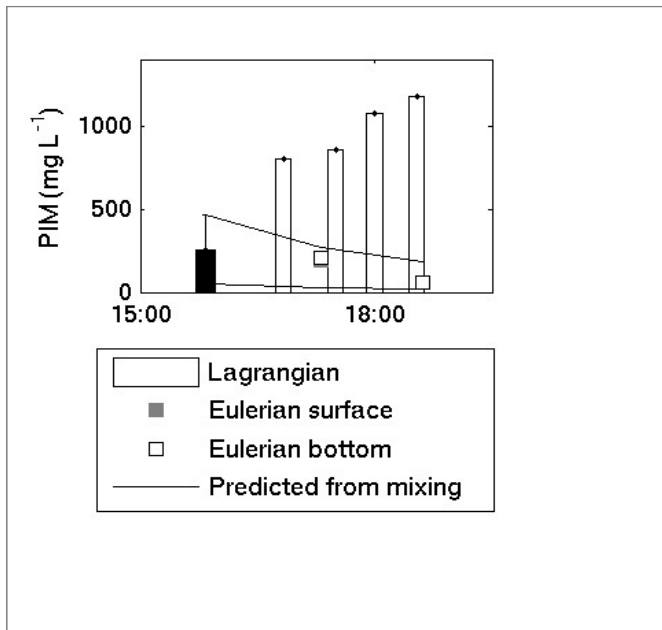


Figure 4

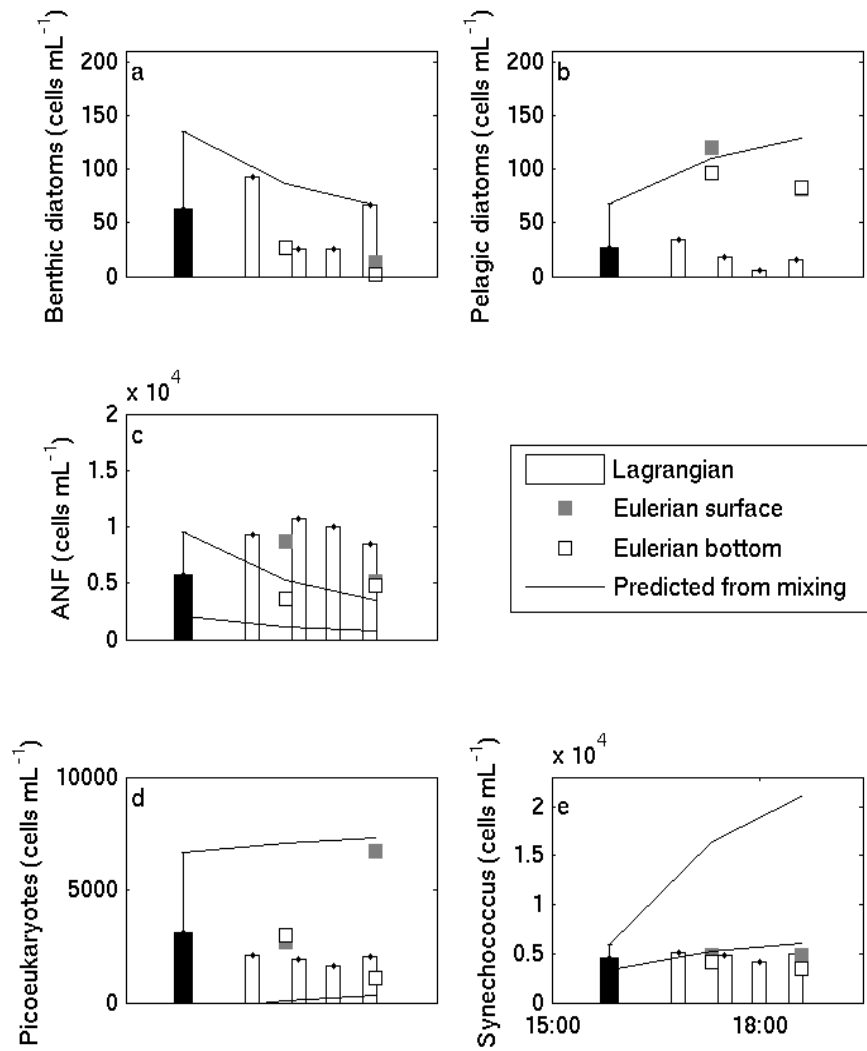


Figure 5

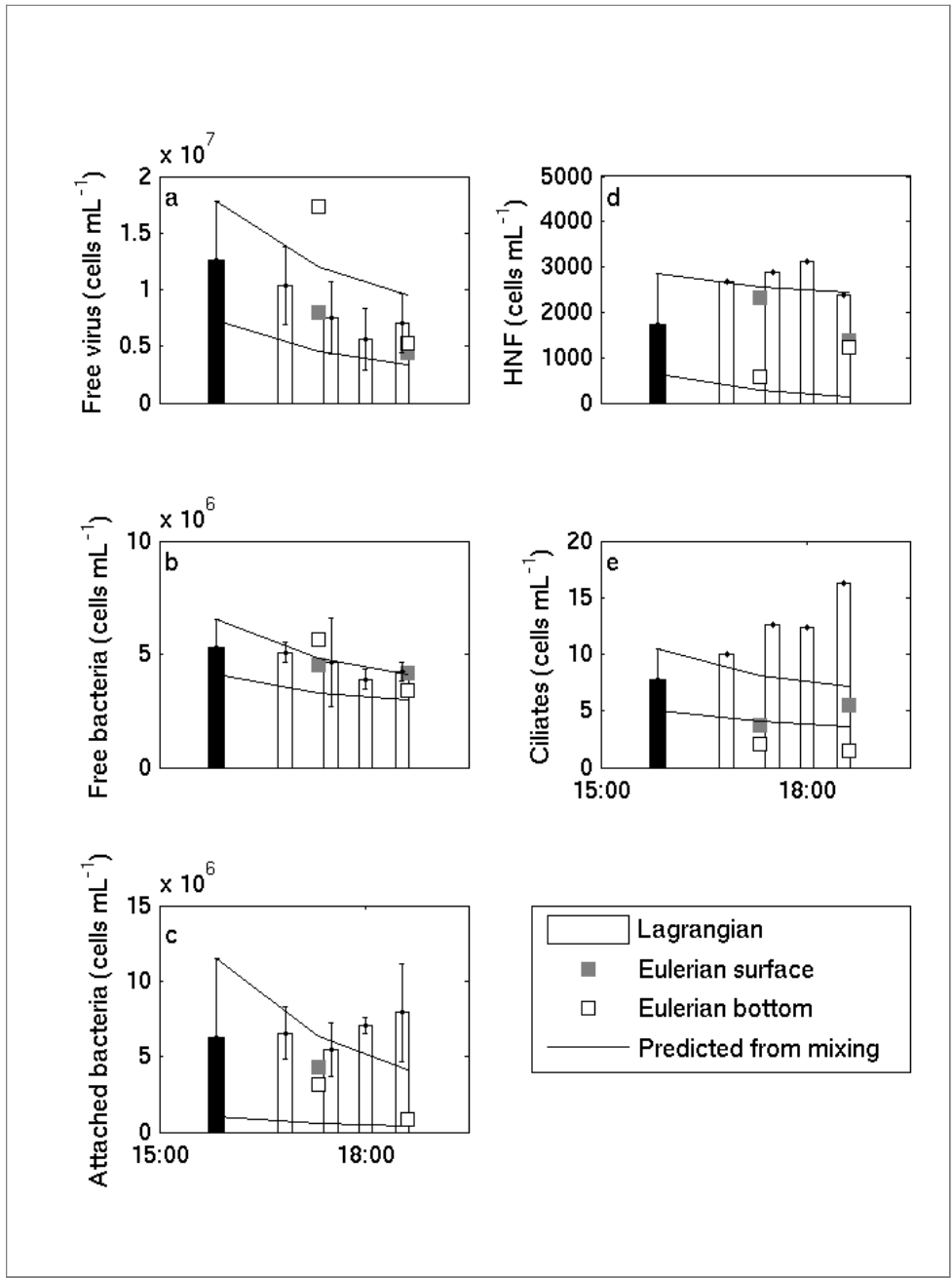


Figure 6

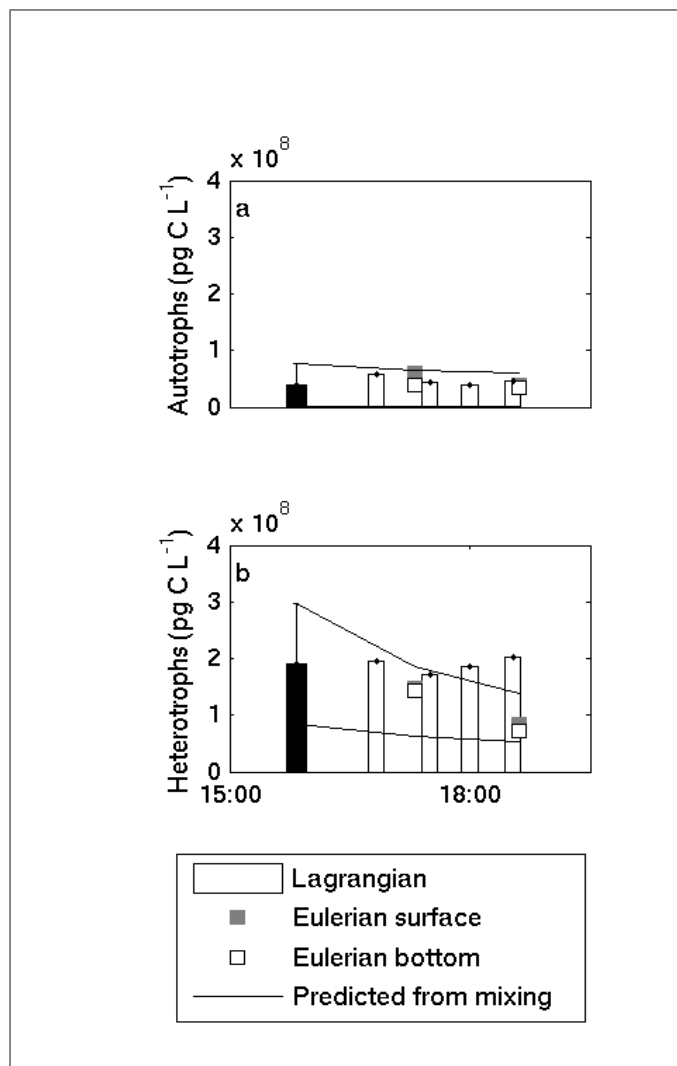


Figure 7